



Long-term and short-term inorganic carbon reservoirs in Aegean seawater – an experimental study

Fabian Gäb¹, Chris Ballhaus¹, Jan Siemens^{2,3}

¹ Institut für Geowissenschaften, Universität Bonn, Bonn, 53115, Germany

5 ² Institut für Nutzpflanzenwissenschaften und Ressourcenschutz, Bereich Bodenwissenschaften, Universität Bonn, Bonn, 53115, Germany

³ present address: Institut für Bodenkunde und Bodenerhaltung, iFZ, Universität Giessen, Giessen, 35392. Germany

Correspondence to: Fabian Gäb (fgaeb@uni-bonn.de)

10

Abstract. The relevant literature does not explicitly address the fact that there are two fundamentally different inorganic carbon (DIC) reservoirs in seawater; (1) a long-term "background" DIC reservoir that is not in net-transfer equilibrium with the atmosphere, and (2) a short-term "atmospheric" DIC reservoir that is fed by atmospheric pCO₂. In addition, we may define a third
15 "anthropogenic" DIC reservoir that quantifies the increase in DIC since industrialization.

We perform experiments to quantify these reservoirs. We equilibrate Aegean seawater with N₂-O₂ (79:21) gases with variable pCO₂ from < 10 to 100,000 µatm, and pure CO₂ gas. We quantify electrochemically the changes in pH and, by titration and IR spectroscopy, total alkalinity (TA) and dissolved inorganic carbon (DIC) that occur with variations in pCO₂. About 78% of the Aegean DIC
20 is "background", introduced into the Aegean sea by the long-term carbon cycle, i.e. riverine input, remineralization of organic carbon, and hydrothermal CO₂. In terms of concentration and in the short term, this reservoir is independent of atmospheric pCO₂. About 22% of DIC is atmospheric in origin and is in exchange equilibrium with atmospheric pCO₂. The anthropogenic contribution to the atmospheric DIC reservoir is derived by measuring the increase in DIC between 280 (pre-
25 industrial) and 410 µatm (present-day) pCO₂ and quantified at around 26%.

Our experiments also allow projections into the future. It has been suspected that increasing

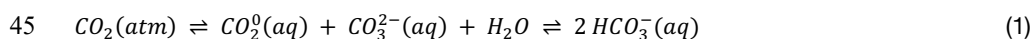


atmospheric $p\text{CO}_2$ lowers the CO_2 absorption capacity of ocean surface water. Our data confirm this assessment. When the $p\text{CO}_2$ increases, the pH and the CO_3^{2-} -concentration fall, and with them the ability of seawater to hydrolyze CO_2 . Without measures to limit anthropogenic CO_2 emissions, the absorption capacity of Aegean seawater in the year 2100 will be only about one half of the absorption capacity of today.

1. Introduction

Emissions of anthropogenic CO_2 not only enhance greenhouse effects in the atmosphere and contribute toward global warming. Atmospheric CO_2 also reacts with ocean surface waters and causes ocean acidification (Caldeira and Duffy 2000, Caldeira and Wickett 2000, Andersson et al. 2005, Andersson et al. 2008, Andersson and Mackenzie 2012, Doney et al. 2009), to an extent that marine organisms may face difficulty in sequestering CaCO_3 to assemble their calcareous shells (Wolf-Gladrow et al. 1999, Riebesell et al. 2000, Caldeira and Wickett 2000, Orr et al. 2005, Guinotte and Fabry 2005).

Thermodynamically it can be calculated how increased CO_2 emissions affect the pH of ocean water (Zeebe and Wolf-Gladrow 2002) and how much CO_2 is exchanged with the atmosphere. Atmospheric CO_2 is physically dissolved, following Henry's law, as $\text{CO}_2^\circ(\text{aq})$ in seawater and then reacts with $\text{CO}_3^{2-}(\text{aq})$ of seawater to $\text{HCO}_3^-(\text{aq})$, according to the equilibria



The hydrolysis of 1 mol CO_2° releases 1 mol H_3O^+ . If pH and another parameter such as total alkalinity (TA) of seawater are known and the anthropogenic fraction of CO_2 of the atmosphere is quantified, then with knowledge of the dissociation constants of H_2CO_3 (Mehrbach et al. 1973; Roy et al. 1993; Dickson and Millero 1987; Wanninkhof et al. 1999, Millero et al. 2006; Millero 2007) we may calculate from eqn. (1) the anthropogenic fraction of dissolved inorganic carbon (DIC) (Zeebe and Wolf-Gladrow 2001, Zeebe and Ridgwell 2011). The practice, however, is more complex since many other factors complicate a quantification. Among them are the mixing rates between shallow ocean water and deep water that is not in equilibrium with atmospheric CO_2 , temperature effects



(warm water dissolves less CO₂ than cold water), regional differences in the mixing rates,
55 photosynthesis, and remineralization of organic carbon. The most widely used methods to quantify
anthropogenic DIC are performed by mass balance calculations (e.g. Sabine et al. 2004, Tanhua et
al. 2007, Gruber et al. 2019, Friedlingstein et al. 2020) and comparative analysis of DIC of deep
ocean water that has not yet seen ingression of anthropogenic CO₂ and other anthropogenic gas
species (Gruber et al. 1996, Na et al. 2022).

60 In this contribution we apply an experimental approach to the problem. We let react natural
seawater with N₂-O₂ (79:21) gases with known quantities of CO₂. We show for the first time that
only a small fraction of the DIC in seawater is in net-transfer equilibrium with the CO₂ of the
atmosphere. By far the largest DIC reservoir in ocean water, around 78%, is inorganic carbon that
was (and is being) derived from the long-term carbon cycle (Berner 1992, 1999), added by
65 weathering reactions, submarine hydrothermal activity, and re-mineralization of organic material.
We refer to this DIC reservoir as "background DIC". The remainder, i.e. ca. 22%, is derived from
the CO₂ exchange between atmosphere and seawater via eqn. (1) and referred to here as
"atmospheric DIC". The anthropogenic fraction of the atmospheric DIC is about 26 ±3%, here
termed "anthropogenic DIC". It corresponds to the DIC fraction added since 1860, the beginning
70 of industrialization, when the pCO₂ was around 280 µatm. We emphasize that all our data and
interpretations are valid only for Aegean seawater.

2. Methods

The seawater used for the equilibration experiments comes from the Aegean sea near the
75 island of Sifnos. Its salinity is determined by ICP-OES analysis at 38‰ NaCl equiv. The Ca²⁺aq
concentration is analyzed at 12 mmol • kg⁻¹. The total alkalinity (TA) is titrated at 2687 ±27 µmol •
kg⁻¹ (2σ). The total DIC (equilibrium with 400 µatm CO₂ partial pressure) is determined by infrared
(IR) spectroscopy (see below) at 2515 ±16 µmol • kg⁻¹ (2σ).

The gases to simulate atmospheric exchange are N₂:O₂ (79:21) gas mixtures with CO₂
80 concentrations of < 10, 200, 280, 410, 1000, 2,000, 5,000, 20,000, and 100,000 µatm CO₂. In



addition, one experiment was performed with pure CO₂ gas. Uncertainties in CO₂ contents are certified by the gas supplier (AirLiquide®) to < 1 relative vol.%. The gases are bubbled through the seawater in 280 ml reaction flasks with gas flow rates of ~ 0.1 L • min⁻¹ (Fig. 1). Temperature is buffered at 25 ± 0.2°C by suspending the flasks in tempered water baths. Equilibration experiments with a near-zero CO₂ gas are carried out at 17°C, in order to suppress, or at least delay, aragonite nucleation (see below). The electromotive force (emf) is monitored with hydrogen ion sensitive glass electrodes using a 3n KCl standard solution as reference electrolyte. The precision is ± 0.02 units in pH. The pH values reported in Table 1 are given on the free hydrogen scale (Dickson 1993). Equilibration between gas and water is assisted by stirring solutions with a magnetic stirrer while they are bubbled with their equilibrium gases. Typical run times are 30 to 50 h. Hydrolysis equilibrium with the gas is considered reached when the pH has remained constant around ± 0.02 pH units for at least 8 hours.

Table 1

pCO ₂ μatm	pH values (n runs)	Total alkalinity μmol kg ⁻¹	HCO ₃ ⁻ μmol kg ⁻¹	CO ₃ ²⁻ μmol kg ⁻¹	CO _{2,aq}	Total CA μmol kg ⁻¹	Total DIC μmol kg ⁻¹
< 10	> 9 (see text) (11)	1630 ± 30 (3)	n/c	n/c	n/c	n/c	1974 ± 27 (11)
200	8,44 ± 0,03 (5)	2714 ± 28 (3)	1798	461	5	2720	2263 ± 19 (9)
280	8,3 ± 0,02 (4)	2631 ± 5 (2)	2019	375	8	2769	2400 ± 8 (11)
410	8,21 ± 0,02 (3)	2687 ± 14 (3)	2177	329	10	2835	2515 ± 16 (36)
700	8,08 ± 0,01 (3)	2634 ± 29 (3)	2392	268	15	2928	2674 ± 38 (9)
1000	7,87 ± 0,07 (10)	2717 ± 24 (6)	2510	174	26	2858	2708 ± 38 (6)
2000	7,55 ± 0,04 (4)	2690 ± 24 (4)	2587	87	55	2761	2727 ± 61 (6)
5000	7,24 ± 0,05 (5)	2732 ± 39 (2)	2642	44	115	2730	2800 ± 78 (6)
20000	6,66 ± 0,01 (4)	2714 ± 7 (11)	2639	13	437	2665	3087 ± 29 (6)
100000	5,97 ± 0,02 (5)	2618 ± 6 (10)	2788	4	2263	2796	5054 ± 52 (6)
1000000	4,94 (1)	1666 (1)	3148	2	27384	3152	30530 ± 300 (3)

Table 1. Summary of the experimental data. Uncertainties quoted are either the analytical ranges (pH and TA) or reflect two standard deviations of the mean (DIC). In parentheses the number of trials (pH), the number of titrations (TA), or the number of samples and aliquots analyzed (DIC). Atmospheric



contributions to DIC are calculated by subtracting from the total DIC at the $p\text{CO}_2$ of interest the DIC at $< 10 \mu\text{atm CO}_2$. Carbon speciations (*) calculated from TA and the pH averages with the stoichiometric constants by Millero et al. (2006). n/a not analyzed, n/c not calculated.

100 Total alkalinities (TA) are titrated in situ, that is, while a seawater sample is bubbled with its
respective equilibrium gas. Titrations are performed with a Metrohm titrator and 0.1 n HCl MerckTM
standard solution. The amount of acid used is equivalent to the TA of the sample, which is set equal
to $[\text{HCO}_3^-] + 2 \cdot [\text{CO}_3^{2-}] + [\text{B}(\text{OH})_4^-] + [\text{OH}^-] + 2 \cdot [\text{PO}_4^{3-}] + [\text{HPO}_4^{2-}] + [\text{SiO}(\text{OH})_3^-] - [\text{H}_3\text{O}^+] - [\text{HSO}_4^-]$.
Titration is continued until a pH of 4.5 is reached. At this pH, all anionic carbon species are
105 considered neutralized to $\text{CO}_{2,\text{aq}}$ and exchanged with the experimental gas. In seawater, between
95 and 97% of the TA are carbonate alkalinity CA (Morse and Mackenzie 1990; Zeebe and Wolf-
Gladrow 2001), defined as $[\text{HCO}_3^-] + 2 \cdot [\text{CO}_3^{2-}] - [\text{H}_3\text{O}^+]$, but it is the total alkalinity that is quantified
by titration.

Following attainment of pH equilibrium, 10 ml aliquots of each solution are siphoned off and
110 analyzed for total DIC. Samples are taken by moving bubble-free solution from the reaction flasks
into rubber-sealed glass vials via PE tubing, using the slight gas overpressure inside the reaction
flasks as driving force. Before samples are taken, the ejection system and the glass vials are vented
with the experimental atmosphere for several minutes and flushed with the equilibrium seawater
solution at least once, to avoid contaminating the water sample with ambient atmosphere. The DIC
115 concentrations are determined with a TOC-VCPH analyzer (Shimadzu Corp.) by extracting solution
from the sealed vials with a headspace-free syringe into a reactor. An aliquot of 25% H_3PO_4 is
injected into the reactor while sparging it with a CO_2 -free carrier gas (purified artificial air). At the pH
imposed by H_3PO_4 (~ 1), all DIC of the sample is liberated as gaseous CO_2 . The CO_2 content in the
carrier gas is then quantified by infrared spectroscopy. The IR spectrometer is calibrated before
120 and after each block of DIC analyses (usually three aliquots of two runs) with four H_2O - NaHCO_3 -
 Na_2CO_3 standard solutions containing 10, 25, 50, and 100 mg C, respectively 833, 2082, 4163, and
8326 $\mu\text{mol DIC per kg water}$. The blank is the DIC in milli-Q water in equilibrium with ambient (410
 μatm) $p\text{CO}_2$, which is calculated with a Henry constant of $3.38 \times 10^{-2} \text{ mol} \cdot \text{L}^{-1} \cdot \text{atm}^{-1}$ at 13.5 μmol
 kg^{-1} DIC. The detection limit is set at three times that blank. For further analytical details see

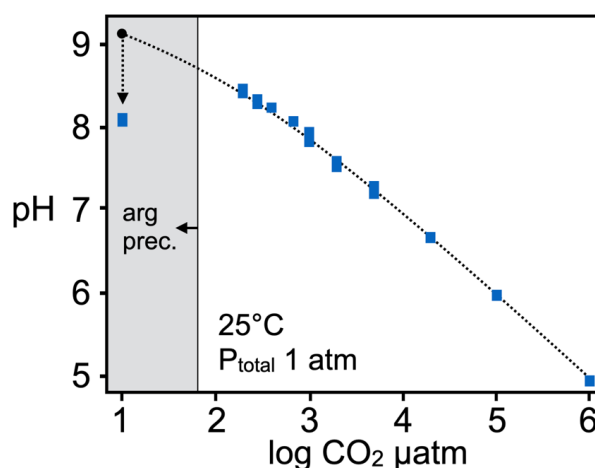


125 Siemens et al. (2012).

3. Results

3.1. Relations between $p\text{CO}_2$ and pH

The pH falls as $p\text{CO}_2$ increases (Fig. 1), in much the same fashion as predicted by
 130 thermodynamic models (Parkhurst 1995, dashed line in Fig. 1). However, there is a $p\text{CO}_2$ - pH
 space, shaded in gray in Fig. 1, where the experiments do not follow the thermodynamically
 calculated trend. The reason is that at a $p\text{CO}_2$ below ca. 50 to 100 μatm CO_2 aragonite is
 precipitated from Aegean seawater, lowering the pH. The issue of aragonite precipitation under low
 $p\text{CO}_2$ will be discussed below.



135 **Figure 1.** The pH of seawater after equilibration with $\text{N}_2:\text{O}_2$ (79:21) artificial gases with variable CO_2
 contents in μatm . The blue symbols are the experimentally determined pH- $p\text{CO}_2$ pairs, the dashed line
 is the pH dependence calculated with PHREEQC (Parkhurst 1995). Symbol lengths reflect the pH range
 of n determinations (cf. Table 1). Uncertainties in terms of $p\text{CO}_2$ as quoted by the gas supplier are ± 10
 μatm in CO_2 . (modified after Gáb et al. 2017)



3.2. Relations between pCO₂ and total alkalinity (TA)

Total alkalinity (TA) in Fig. 2 averages around $2687 \pm 27 \mu\text{mol kg}^{-1}$ (2 σ) and is slightly higher than the alkalinity of Mediterranean seawater reported by Schneider et al. (2007) at $2600 \mu\text{mol kg}^{-1}$.

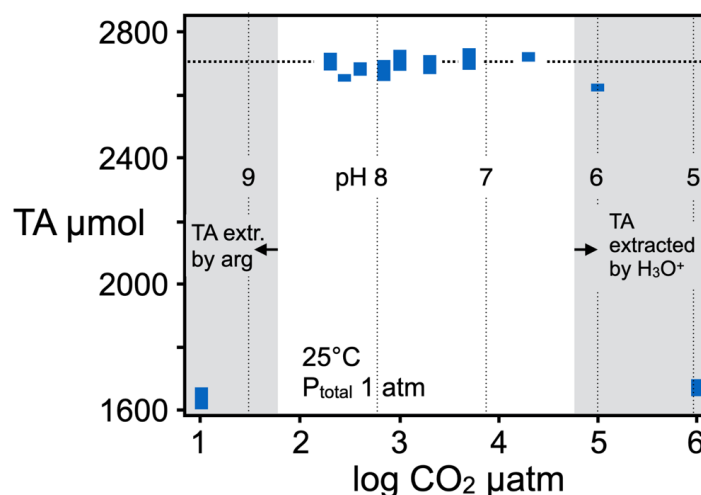


Figure 2. Total alkalinity (TA) of the seawater in $\mu\text{mol} \cdot \text{kg}^{-1}$, titrated with 0.1 n HCl while each water sample was kept in exchange equilibrium with its respective gas. Blue symbols experimental data, dashed line (Parkhurst 1995) to illustrate that TA is considered independent of pCO₂ (Millero 2005, Zeebe and Wolf-Gladrow 2001). Numbers next to symbols are the pH values from Table 1. Error bars are the ranges of n titrations. (modified after Gáb et al. 2017)

Contrary to statements in the literature (Morse and Mackenzie, 1990; Zeebe and Wolf-Gladrow 2001), the TA of seawater is not strictly independent of pCO₂: below a CO₂ of ca. 50 to 100 μatm , the pH and the HCO₃⁻/CO₃²⁻ ratio in solution adopt values so high (respectively so low) that Aegean seawater precipitates aragonite, lowering TA by CaCO₃ extraction to $1630 \pm 30 \mu\text{mol kg}^{-1}$. At very high pCO₂, that is, when CO₂ exceeds 100,000 μatm , the H₃O⁺ concentration generated by the hydrolysis of CO₂ (eqn. 1) is high enough to neutralize some HCO₃⁻ to CO₂ (aq) and drive it out with the experimental gas. In Fig. 2, the two regions where TA is not independent of pH are shaded in grey. Obviously though, these two regions are of theoretical interest only, for neither in the past nor in the foreseeable future were (or will) CO₂ < 50 to 100 and CO₂ > 100,000 μatm be reached. Nonetheless, the statement that the TA is independent of pCO₂ (Zeebe and Wolf-Gladrow 2001) is



160 not strictly valid for the entire range of possible CO_2 partial pressures.

3.3. Relations between pCO_2 and dissolved inorganic carbon (DIC)

Total DIC as analyzed with IR spectroscopy is shown in Fig. 3. For comparison we also display the DIC of fresh water at 25°C calculated with Henry's law and a K_H of $3.38 \cdot 10^{-2} \text{ mol} \cdot \text{L}^{-1}$

165 $\cdot \text{atm}^{-1}$ (dashed line).

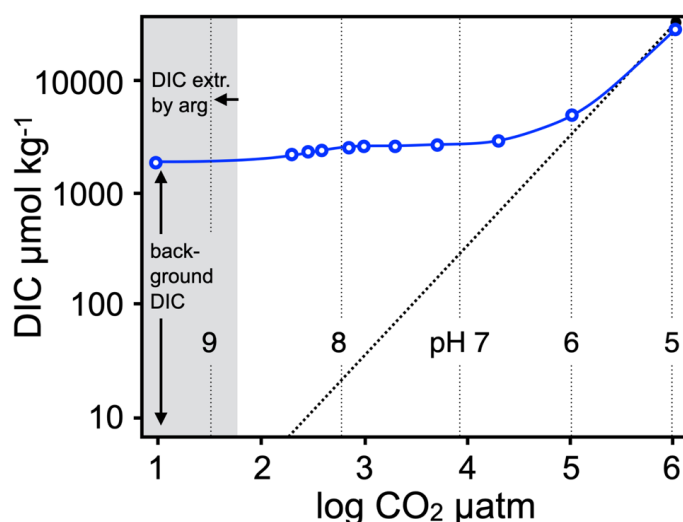


Figure 3. Total dissolved inorganic carbon (DIC) versus the CO_2 partial pressures of the experimental gases, in Aegean seawater (blue curve 1) and in fresh water (dashed line). At low pCO_2 , CO_2 is dissolved by hydrolysis via eqn. (1) while above a pCO_2 of $\sim 5,000 \mu\text{atm}$ dissolution is increasingly physical by $\text{CO}_{2,\text{atm}} \rightleftharpoons \text{CO}_{2,\text{aq}}$. The CO_2 uptake by pure water is calculated with a Henry constant $K_H = 3.38 \cdot 10^{-2} \text{ mol kg}^{-1} \text{ atm}^{-1}$. (modified after Gáb et al. 2017)

With increasing pCO_2 , DIC increases as expected, although the actual dependence between the two parameters is found relatively small. While pCO_2 of the gas phase increases from 200 to 1,000,000 μatm by a factor of 5000, the DIC in the equilibrium seawater is only raised by a factor of 15.5. That is due to the high background DIC, i.e. that fraction that is not extractable by changing pCO_2 . The amount of background corresponds to the difference in DIC between Aegean seawater



and fresh water (arrow in Fig. 3). In the low $p\text{CO}_2$ region, below a $p\text{CO}_2$ of $\sim 5,000 \mu\text{atm}$, carbon is dissolved by hydrolysis (eqn. 1), while above a $p\text{CO}_2$ of $\sim 10,000 \mu\text{atm}$ dissolution is increasingly physical by $\text{CO}_{2,\text{gas}} \rightleftharpoons \text{CO}_{2,\text{aq}}$.

180 Considerable effort went into determining experimentally the background DIC fraction, entrained into the oceans by processes governing the long-term carbon cycle (Berner 1999). Experimentally, it would seem straightforward to determine that fraction by difference, once all exchangeable DIC is extracted from the water by equilibration of with a zero- CO_2 gas. However, this involves experimental problems. When a seawater solution is exposed to near-zero $p\text{CO}_2$ (here $< 10 \mu\text{atm}$
185 CO_2 , Table 1), the pH and the ion concentration product $[\text{Ca}^{2+}] \cdot [\text{CO}_3^{2-}]$ of the water rise with exposure time until a pH is reached where the supersaturation in CaCO_3 of Aegean seawater becomes so high that aragonite precipitates, extracting both TA and DIC.

When solid CaCO_3 is stabilized, the solutions become turbid, precipitating a whitish phase. Phase analysis by XRD characterizes the precipitate as aragonite, and SEM imaging identifies star-
190 shaped aragonite aggregates with μm -sized aragonite crystals arranged radially around a nucleus (Fig. 4). Aggregates similar in morphology may be seen in the cores of aragonite ooids observed at the Bahama banks (Dravis 1979; Rankey and Reeder 2009; 2010). This is not to say that whitenings in the Bahamas are triggered by a drop in $p\text{CO}_2$ but unusually high water temperatures could have a similar effect, since warmer water cannot dissolve as much CO_2 .

195



10

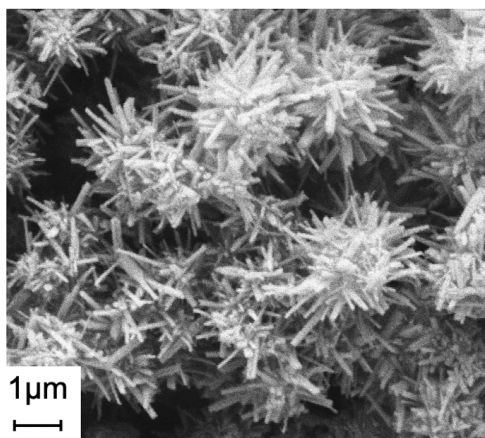


Figure 4. Secondary electron image of aragonite aggregates, precipitated from Aegean seawater while it is reacted with a zero-CO₂ (pCO₂ < 10 μatm) gas.

Given those results, it is clear that reliable pH, TA or DIC values can no longer be determined with aragonite in suspension. We try to overcome the problem of aragonite precipitation with time series runs. While a water sample is reacted with a near-zero (< 10 μatm) CO₂ gas, 10 ml water samples are taken from the reaction flasks in regular intervals (several hours) until aragonite precipitation is observed. To delay aragonite precipitation, these time series experiments are carried out at 17 instead of the usual 25°C equilibration temperature. The expectation is that a slightly lower temperature may help keep aragonite metastably in solution, hence may delay the onset of aragonite nucleation to a higher pH and extend the pH-pCO₂ range within which aragonite-free low-pCO₂ water samples can be taken.

One such time series is shown in Fig. 5. The degree of aragonite saturation is computed in terms of Ω_{arg} , which is defined as the $[\text{Ca}^{2+}] \cdot [\text{CO}_3^{2-}]$ ion concentration product in seawater divided by the stoichiometric solubility product of aragonite ($6.65 \pm 0.12 \cdot 10^{-7} \text{ mol}^2 \text{ kg}^{-2}$, Mucci 1983). As expected, Ω_{arg} increases with exposure time to a near-zero CO₂ gas. When pH rises, the HCO₃⁻



$\text{HCO}_3^-/\text{CO}_3^{2-}$ ratio falls and Ω_{arg} increases.

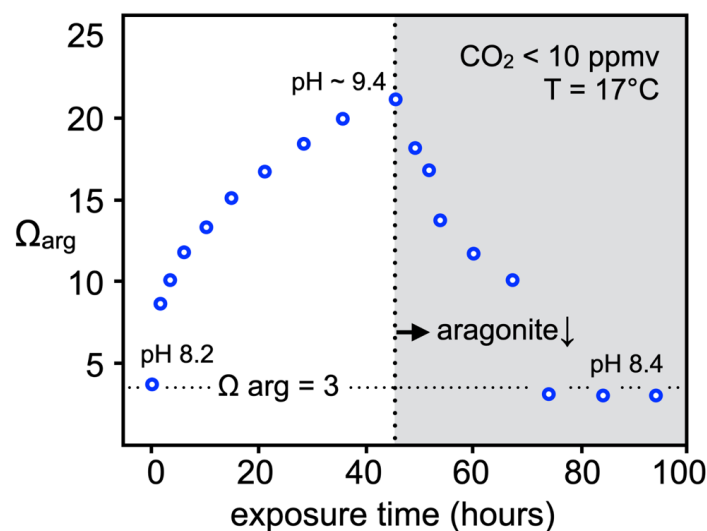


Figure 5. Time series experiments with $\text{pCO}_2 < 10 \mu\text{atm}$ at 17°C , carried out to semi-quantify the background DIC. Region where macroscopic aragonite saturation is observed is shaded in grey. Note that after aragonite precipitation, Ω_{arg} finds back to a value near 3, identical to Ω_{arg} of pristine Aegean seawater (see text).

Spontaneous precipitation is usually observed when the pH has reached a value near 9.4, which for Aegean seawater corresponds to a $\text{HCO}_3^-/\text{CO}_3^{2-}$ concentration ratio of $\sim 2.5 : 1$ calculated with PHREEQC (Mehrbach et al. 1973; Dickson and Millero 1987; Pankhurst 1995; Table 1). After aragonite has settled out and the solution has cleared, the TA of the remaining solution is titrated at $\sim 1630 \pm 30 \mu\text{mol kg}^{-1}$. The pH also falls when aragonite is extracted, from ca. 9.4 to 8.4. The loss in TA after aragonite precipitation compared to pristine Aegean seawater at $\text{pCO}_2 = 410 \mu\text{atm}$ ($\text{TA} = 2687 \mu\text{mol} \cdot \text{kg}^{-1}$) is about 40%.

We note with interest that following aragonite precipitation, the residual solution finds back to an Ω_{arg} of ~ 3 , near-identical to the Ω_{arg} of pristine Aegean seawater prior to exposure to a near-zero pCO_2 gas (Fig. 5). Intuitively, one would expect Ω_{arg} to drop to unity when macroscopic aragonite falls, i.e. that the intrinsic aragonite oversaturation of Aegean seawater would be degraded as well. However, this does not seem to be the case. Perhaps the study by Gebauer et



al. (2008) provides an explanation: these authors found that Ca^{2+} and CO_3^{2-} tend to form stable prenucleation clusters even when a solution is CaCO_3 undersaturated. Apparently, this fraction of cluster CaCO_3 in seawater is not affected by the precipitation reaction in Fig. 5, but is retained even when macroscopic aragonite precipitates.

The average DIC of 11 zero- CO_2 analyzed seawater samples, reacted at 17°C and drawn just before aragonite precipitation set in, is analyzed at 1974 ± 27 (2σ) $\mu\text{mol C per kg seawater}$ (Table 1). This is our best estimate as to the background DIC in Aegean seawater, added by processes of the long-term carbon cycle. Note that despite all experimental efforts in delaying aragonite precipitation, this DIC concentration may still be a maximum. In CaCO_3 oversaturated seawater, DIC equilibrium with a zero- CO_2 gas can only be approached but never precisely reached.

4. Discussion

4.1. The inorganic carbon inventory of Mediterranean seawater

Our data allow to differentiate for the first time quantitatively among the inorganic carbon contributions to Aegean seawater and seawater in general. Around $1974 \pm 27 \mu\text{mol kg}^{-1}$, or 78% of the total DIC at ambient pCO_2 , are background DIC. That fraction is quantified by reacting seawater with near-zero CO_2 gas and recording the pH at which aragonite precipitation begins ($\text{pH} \sim 9.4$). The background DIC value resulting must be a maximum, for we cannot rule out the possibility that samples are contaminated by small amounts of suspended aragonite crystals. To determine an accurate value, equilibrium with a zero- CO_2 gas would be needed, but this is not possible since Aegean seawater is supersaturated with respect to CaCO_3 . In the land-locked Aegean sea without active spreading ridges, the principal sources are surface weathering and remineralization of organic carbon, less so hydrothermal input.

In terms of bulk concentration, the background DIC fraction is not in net-transfer exchange with the atmosphere and independent of short-term variations in atmospheric CO_2 . This means that short-term variations in pCO_2 do not alter the concentration of background DIC. In terms of speciation, however, the background fraction does respond to changes in pCO_2 by changing its



255 $\text{HCO}_3^-/\text{CO}_3^{2-}$ ratio when pCO_2 and pH fluctuate. An analogue to this behavior is the sulfate SO_4^{2-}
concentration in seawater ($\sim 29 \text{ mmol} \cdot \text{kg}^{-1}$; Millero 2005). Sulfate is also out of net transfer
equilibrium with the SO_2 of the present-day pristine atmosphere (Berner 2004) which carries \sim
 $0.0036 \mu\text{atm SO}_2$ (DWD 2022). Sulfate in seawater probably originates from oxidative weathering of
260 sulfide, just as background DIC is contributed by surface weathering, hydrothermal input, and
remineralization of organic matter. In the long term though, background DIC is not inert to
atmospheric CO_2 , as this reservoir is influenced by processes like CaCO_3 solution-precipitation and
photosynthesis. However, these processes operate on much longer time scales of up to millions of
years (Berner 2003) than CO_2 air-sea exchange (cf. Sabine and Tanhua 2010).

The DIC fraction in Aegean seawater that is exchangeable with the atmosphere at present-
265 day atmospheric CO_2 level is quantified analytically at $540 \mu\text{mol kg}^{-1}$, or 22% of the total DIC. This
fraction is given by the DIC difference between the background DIC and the DIC analyzed at 410
 $\mu\text{atm CO}_2$ (Table 1). The anthropogenic fraction of this exchangeable DIC is $115 \mu\text{mol} \cdot \text{kg}^{-1}$. This
fraction is calculated by measuring the DIC increase between 280 and $410 \mu\text{atm CO}_2$ and relating
it to the bulk atmospheric DIC at $410 \mu\text{atm CO}_2$. The result is that $26 \pm 3\%$ of the atmospheric DIC
270 must be anthropogenic in origin.

4.2. Comparison with other studies

Our anthropogenic DIC fraction ($26 \pm 3\%$) compares quite favorably with other
275 quantifications from the literature, although it is valid only for Aegean seawater. Gruber et al. (1996)
approximate the uptake of northern and tropical Atlantic waters between 1980 and 1989 with ca.
30% of anthropogenic CO_2 . They derive that fraction by comparing the DIC of deep water
uncontaminated by anthropogenic CO_2 with the DIC of surface waters. Sabine et al. (2004) calculate
via mass balance that global oceans absorbed from 1800 to 1999 ca. 48%, and from 1980 to 1999
280 ca. 30% anthropogenic CO_2 . The difference implies that with increasing CO_2 and time the
absorption capacity may diminish (see below). Sabine and Tanhua (2010) quote the oceanic uptake



as ~ 25% CO₂. Gruber et al. (2019) calculate via mass balance the anthropogenic share of DIC for the time interval from 1994 to 2007 as 34 ± 4 Gt via mass balance which corresponds to ~ 31 ± 4% of total emitted CO₂. Friedlingstein et al. (2020) calculate, again by mass balance (cf. eqn. 1 in their paper) that from 2010 to 2019 about 22% of the anthropogenic CO₂ emissions were absorbed by ocean water. We do not wish to imply that our value is more accurate than that of previous studies, especially since it is only valid for Aegean seawater. However, it does give credence to our purely experimental approach when we derive, without the intrinsic uncertainties in quantifying all terrestrial carbon reservoirs, an anthropogenic fraction that agrees well with literature data.

290

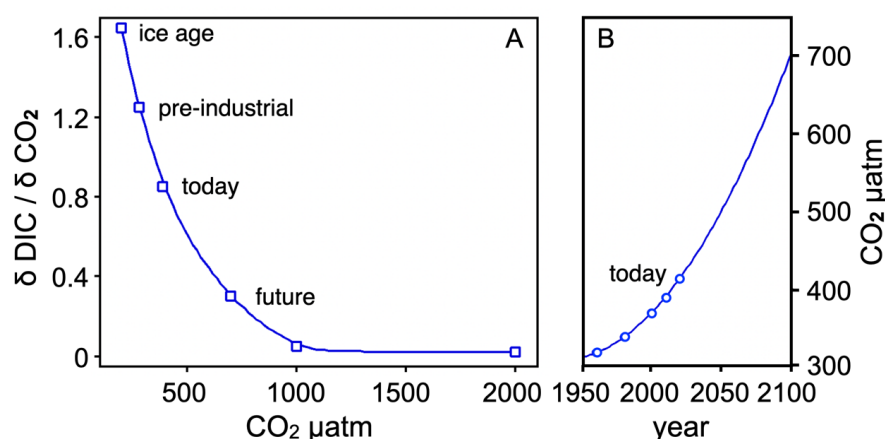
4.3. Future development

Our data also allow an assessment of whether the percent uptake of CO₂ by ocean water will remain constant or change with time and increasing pCO₂. There is already the suspicion that the uptake capacity decreases with time with increasing anthropogenic pCO₂ (Sarmiento et al. 2000, Knorr 2009; Orr 2013). Sabine and Tanhua (2010) note that "the rate of ocean carbon uptake does not seem to be keeping pace with the rate of growth in CO₂ emissions". We support this assessment. For once, it is only the top several 100s of meters of ocean water above the thermocline that is an effective CO₂ sink, and that reservoir could "fill up" over time because the mixing rate with deep water does not keep pace with CO₂ uptake by hydrolysis (cf. Sabine et al. 2004). Second, as pCO₂ increases, the HCO₃⁻/CO₃²⁻ rises, thereby reducing the uptake capacity of CO₂ via eqn. (1). Third, with increasing pCO₂ due to anthropogenic emissions, the average temperature of seawater (above the thermocline) will increase, and thus the capacity to absorb CO₂ will diminish since warm water dissolves less CO₂ than cold water.

300



We concur with Sarmiento et al. (2000), Sabine et al. (2004), Knorr (2009), Sabine and
 305 Tanhua (2010), and Orr (2013) that with time and increasing CO₂ emissions, the uptake capacity of
 seawater will degrade. In Fig. 6a, we show the change in DIC with CO₂ of the atmosphere. In effect,
 the vertical axis of Fig. 6a is the inverse of the Revelle factor (Revelle and Suess, 1957; Egleston et
 al. 2010), defined as $(\Delta\text{CO}_2/\text{CO}_2)/(\Delta\text{DIC}/\text{DIC})$ where ΔCO_2 and ΔDIC denote the differences in pCO₂
 and DIC from today's values (410 μatm CO₂; Table 1).



310 **Figure 6. Absorption capacity of anthropogenic CO₂ by Aegean seawater (A) and potential increase in
 pCO₂ by extrapolation of the monthly Mauna Loa averages to the year 2100 (B). For details see text.**

The graph suggests that in the near future the shallow regions of the Aegean ocean in exchange
 equilibrium with the atmosphere may fill up with respect to anthropogenic DIC. If CO₂ emissions
 continue to increase as projected in Fig. 6b, the buffering capacity in 2100 (700 μatm) would be
 315 reduced by more than half compared to today. In addition, there is a temperature effect with global
 warming since warm seawater dissolves less CO₂. Not taken into account in Fig. 6a are the mixing
 rates between shallow water and deep water, but the latter occur at much longer timescales than
 the equilibration of seawater with atmospheric CO₂ (cf. Caldeira and Wickett 2003).

320 5. Conclusions and Implications

We have equilibrated natural seawater from the Aegean sea with N₂-O₂ gases with variable



pCO₂ and determined pH, TA and DIC as a function of pCO₂. The experiments allow to identify and quantify the different DIC reservoirs in seawater. There are two principal reservoirs; (1) background DIC that is introduced via the long-term carbon cycle and that is not in net-transfer equilibrium with the pCO₂ of the atmosphere, and (2) an atmospheric DIC reservoir that is fed by the pCO₂ of the atmosphere. The percentages of these two reservoirs in Aegean seawater are about 78 and 22%, respectively. To our knowledge, it is the first time that these two reservoirs are explicitly distinguished and quantified.

We quantify the fraction of anthropogenic DIC that has entered Aegean seawater since industrialization. The increase in anthropogenic CO₂ between a pCO₂ of 280 and 410 µatm is 26 ± 3% of the atmospheric DIC. In the future, the uptake capacity may fall if CO₂ emissions continue as before and if the exchange rate between surface ocean water and deep water does not change with global warming. A further increase in pCO₂ decreases the HCO₃⁻/CO₃²⁻-ratio and depletes seawater in the carbonate ion, which is essential for the hydrolysis of atmospheric CO₂ (eqn. 1).

Following the studies by Gebauer et al. (2008, 2014) we suggest that some of the Ca²⁺ and CO₃²⁻ in seawater must be present in the form of associated nano-sized pre-nucleation clusters. Even when macroscopic aragonite precipitates, we note that the supersaturation in CaCO₃ persists and that the left-over solute after aragonite precipitation reverts to an Ω_{arg} of ~ 3 (cf. Fig. 6). This is more important than it seems. Perhaps we can generalize to the extent by stating that the CaCO₃ supersaturation of seawater is due to CaCO₃ nano-particles. This could be beneficial for marine calcifying organisms. Normally it is assumed that calcifiers extract Ca²⁺ hydrates (Ca²⁺(H₂O)_x) and CO₃²⁻ ions from seawater to build their CaCO₃ skeletons or shells (cf. de Nooijer et al. 2012 and refs therein), but energetically it may be more advantageous to use already existing stable nano-nuclei as building materials rather than ionic species. In this context, it is important that Gebauer et al. (2008, 2014) noted CaCO₃ nanoparticles to remain stable even when a solution is CaCO₃ undersaturated (Ω_{arg} < 1). By implication, it may follow that carbonate accreting marine organisms can handle ocean acidification better than is widely assumed (cf. Wolf-Gladrow et al. 2001, Gattuso and Hansson 2011, Riebesell and Tortell 2011).



350 Acknowledgments

The experimental and analytical setup benefited from many helpful suggestions by Bruno Barbier, Henrik Blanchard, and the machine shop of the Institute. Georg Oleschinsky helped with the SEM work, Minh-Chi Tran-Thi assisted in analyzing samples for DIC, Bruno Barbier analyzed the precipitates with XRD, Ashlea Wainwright and Sebastian Lüning commented on the manuscript.

355 Funding by the German Research Council (DFG) to C. Ballhaus through grant Ba 964/31 is acknowledged.

References

- 360 1. Andersson, A. and Mackenzie, F.: Revisiting four scientific debates in ocean acidification research, 9, 893–905, 2012.
2. Andersson, A. J., Mackenzie, F. T., and Lerman, A.: Coastal ocean and carbonate systems in the high CO₂ world of the Anthropocene, 305, 875–918, 2005.
3. Andersson, A. J., Mackenzie, F. T., and Bates, N. R.: Life on the margin: implications of ocean acidification on Mg-calcite, high latitude and cold-water marine calcifiers, 373, 265–273, 2008.
- 365 4. Wetter und Klima - Deutscher Wetterdienst - Sulfur dioxide (SO₂): https://www.dwd.de/EN/research/observing_atmosphere/composition_atmosphere/trace_gases/cont_nav/so2_node.html, last access: 9 May 2022.
5. Berner, R. A.: Weathering, plants, and the long-term carbon cycle, 56, 3225–3231, 1992.
- 370 6. Berner, R. A.: The long-term carbon cycle, fossil fuels and atmospheric composition, 426, 323–326, 2003.
7. Berner, R. A.: A model for calcium, magnesium and sulfate in seawater over Phanerozoic time, 304, 438–453, 2004.
8. Berner, R. A. and others: A new look at the long-term carbon cycle, 9, 1–6, 1999.



- 375 9. Caldeira, K. and Duffy, P. B.: The role of the Southern Ocean in uptake and storage of anthropogenic carbon dioxide, 287, 620–622, 2000.
10. Caldeira, K. and Wickett, M. E.: Anthropogenic carbon and ocean pH, 425, 365–365, 2003.
11. Dickson, A. and Millero, F. J.: A comparison of the equilibrium constants for the dissociation of carbonic acid in seawater media, 34, 1733–1743, 1987.
- 380 12. Dickson, A. G.: pH buffers for sea water media based on the total hydrogen ion concentration scale, 40, 107–118, 1993.
13. Doney, S. C., Fabry, V. J., Feely, R. A., and Kleypas, J. A.: Ocean acidification: the other CO₂ problem, 1, 169–192, 2009.
14. Dravis, J.: Rapid and widespread generation of Recent oolitic hardgrounds on a high energy
385 Bahamian platform, Eleuthera Bank, Bahamas, 49, 195–207, 1979.
15. Egleston, E. S., Sabine, C. L., and Morel, F. M.: Revelle revisited: Buffer factors that quantify the response of ocean chemistry to changes in DIC and alkalinity, 24, 2010.
16. Friedlingstein, P., O’Sullivan, M., Jones, M. W., Andrew, R. M., Hauck, J., Olsen, A., Peters, G. P., Peters, W., Pongratz, J., Sitch, S., Le Quéré, C., Canadell, J. G., Ciais, P., Jackson, R. B.,
390 Alin, S., Aragão, L. E. O. C., Armeth, A., Arora, V., Bates, N. R., Becker, M., Benoit-Cattin, A., Bittig, H. C., Bopp, L., Bultan, S., Chandra, N., Chevallier, F., Chini, L. P., Evans, W., Florentie, L., Forster, P. M., Gasser, T., Gehlen, M., Gilfillan, D., Gkritzalis, T., Gregor, L., Gruber, N., Harris, I., Hartung, K., Haverd, V., Houghton, R. A., Ilyina, T., Jain, A. K., Joetzjer, E., Kadono, K., Kato, E., Kitidis, V., Korsbakken, J. I., Landschützer, P., Lefèvre, N., Lenton, A., Lienert, S., Liu, Z.,
395 Lombardozi, D., Marland, G., Metzl, N., Munro, D. R., Nabel, J. E. M. S., Nakaoka, S.-I., Niwa, Y., O’Brien, K., Ono, T., Palmer, P. I., Pierrot, D., Poulter, B., Resplandy, L., Robertson, E., Rödenbeck, C., Schwinger, J., Séférian, R., Skjelvan, I., Smith, A. J. P., Sutton, A. J., Tanhua, T., Tans, P. P., Tian, H., Tilbrook, B., van der Werf, G., Vuichard, N., Walker, A. P., Wanninkhof, R., Watson, A. J., Willis, D., Wiltshire, A. J., Yuan, W., Yue, X., and Zaehle, S.: Global Carbon
400 Budget 2020, 12, 3269–3340, <https://doi.org/10.5194/essd-12-3269-2020>, 2020.



17. Gäb, F., Ballhaus, C., Siemens, J., Heuser, A., Lissner, M., Geisler, T., and Garbe-Schönberg, D.: Siderite cannot be used as CO₂ sensor for Archaean atmospheres, 214, 209–225, <http://dx.doi.org/10.1016/j.gca.2017.07.027>, 2017.
18. Gattuso, J.-P. and Hansson, L.: Ocean acidification: background and history, 1–20, 2011.
- 405 19. Gebauer, D., Volkel, A., and Colfen, H.: Stable prenucleation calcium carbonate clusters, 322, 1819–1822, 2008.
20. Gebauer, D., Kellermeier, M., Gale, J. D., Bergström, L., and Cölfen, H.: Pre-nucleation clusters as solute precursors in crystallisation, 43, 2348–2371, 2014.
21. Gruber, N., Sarmiento, J. L., and Stocker, T. F.: An improved method for detecting
410 anthropogenic CO₂ in the oceans, 10, 809–837, 1996.
22. Gruber, N., Landschützer, P., and Lovenduski, N. S.: The variable Southern Ocean carbon sink, 11, 159–186, 2019a.
23. Gruber, N., Landschützer, P., and Lovenduski, N. S.: The Variable Southern Ocean Carbon Sink, 11, 159–186, <https://doi.org/10.1146/annurev-marine-121916-063407>, 2019b.
- 415 24. Guinotte, J. M. and Fabry, V. J.: Ocean acidification and its potential effects on marine ecosystems, 1134, 320–342, 2008.
25. Knorr, W.: Is the airborne fraction of anthropogenic CO₂ emissions increasing?, 36, 2009.
26. Mehrbach, C., Culberson, C., Hawley, J., and Pytkowicz, R.: Measurement of the apparent dissociation constants of carbonic acid in seawater at atmospheric pressure 1, 18, 897–907,
420 1973.
27. Millero, F. J.: Chemical oceanography, CRC press, 2005.
28. Millero, F. J.: The marine inorganic carbon cycle, 107, 308–341, 2007.
29. Millero, F. J., Graham, T. B., Huang, F., Bustos-Serrano, H., and Pierrot, D.: Dissociation constants of carbonic acid in seawater as a function of salinity and temperature, 100, 80–94,
425 2006.



30. Morse, J. W. and Mackenzie, F. T.: Geochemistry of sedimentary carbonates, Elsevier, 1990.
31. Mucci, A. and others: The solubility of calcite and aragonite in seawater at various salinities, temperatures, and one atmosphere total pressure, 283, 780–799, 1983.
32. Na, T., Hwang, J., Kim, S.-Y., Jeong, S., Rho, T., and Lee, T.: Large Increase in Dissolved
430 Inorganic Carbon in the East Sea (Japan Sea) From 1999 to 2019, 9,
<https://doi.org/10.3389/fmars.2022.825206>, 2022.
33. de Nooijer, L. J., Toyofuku, T., and Kitazato, H.: Foraminifera promote calcification by elevating their intracellular pH, 106, 15374–15378, 2009.
34. Orr, J. C.: Recent and future changes in ocean carbonate chemistry, 1, 41–66, 2011.
- 435 35. Orr, J. C., Fabry, V. J., Aumont, O., Bopp, L., Doney, S. C., Feely, R. A., Gnanadesikan, A., Gruber, N., Ishida, A., Joos, F., and others: Anthropogenic ocean acidification over the twenty-first century and its impact on calcifying organisms, 437, 681–686, 2005.
36. Parkhurst, D. L.: User's guide to PHREEQC: A computer program for speciation, reaction-path, advective-transport, and inverse geochemical calculations, US Department of the Interior, US
440 Geological Survey, 1995.
37. Rankey, E. C. and Reeder, S. L.: Holocene ooids of Aitutaki Atoll, Cook Islands, South Pacific, 37, 971–974, 2009.
38. Rankey, E. C. and Reeder, S. L.: Controls on platform-scale patterns of surface sediments, shallow Holocene platforms, Bahamas, 57, 1545–1565, 2010.
- 445 39. Revelle, R. and Suess, H. E.: Carbon dioxide exchange between atmosphere and ocean and the question of an increase of atmospheric CO₂ during the past decades, 9, 18–27, 1957.
40. Riebesell, U. and Tortell, P. D.: Effects of ocean acidification on pelagic organisms and ecosystems, 99–121, 2011.
41. Riebesell, U., Zondervan, I., Rost, B., Tortell, P. D., Zeebe, R. E., and Morel, F. M.: Reduced
450 calcification of marine plankton in response to increased atmospheric CO₂, 407, 364–367,



- 2000.
42. Roy, R. N., Roy, L. N., Vogel, K. M., Porter-Moore, C., Pearson, T., Good, C. E., Millero, F. J.,
and Campbell, D. M.: The dissociation constants of carbonic acid in seawater at salinities 5 to
45 and temperatures 0 to 45°C, 44, 249–267, [https://doi.org/10.1016/0304-4203\(93\)90207-5](https://doi.org/10.1016/0304-4203(93)90207-5),
455 1993.
43. Sabine, C. L. and Tanhua, T.: Estimation of Anthropogenic CO₂ Inventories in the Ocean, 2,
175–198, <https://doi.org/10.1146/annurev-marine-120308-080947>, 2010.
44. Sabine, C. L., Feely, R. A., Gruber, N., Key, R. M., Lee, K., Bullister, J. L., Wanninkhof, R., Wong,
C. S., Wallace, D. W. R., Tilbrook, B., Millero, F. J., Peng, T.-H., Kozyr, A., Ono, T., and Rios, A.
460 F.: The Oceanic Sink for Anthropogenic CO₂, 305, 367–371,
<https://doi.org/10.1126/science.1097403>, 2004.
45. Sarmiento, J. L., Monfray, P., Maier-Reimer, E., Aumont, O., Murnane, R. J., and Orr, J. C.: Sea-
air CO₂ fluxes and carbon transport: A comparison of three ocean general circulation models,
14, 1267–1281, <https://doi.org/10.1029/1999GB900062>, 2000.
- 465 46. Schneider, A., Wallace, D. W. R., and Körtzinger, A.: Alkalinity of the Mediterranean Sea, 34,
<https://doi.org/10.1029/2006GL028842>, 2007.
47. Tanhua, T., Körtzinger, A., Friis, K., Waugh, D. W., and Wallace, D. W. R.: An estimate of
anthropogenic CO₂ inventory from decadal changes in oceanic carbon content, 104, 3037–
3042, <https://doi.org/10.1073/pnas.0606574104>, 2007a.
- 470 48. Tanhua, T., Körtzinger, A., Friis, K., Waugh, D. W., and Wallace, D. W. R.: An estimate of
anthropogenic CO₂ inventory from decadal changes in oceanic carbon content, 104, 3037–
3042, <https://doi.org/10.1073/pnas.0606574104>, 2007b.
49. Wanninkhof, R., Lewis, E., Feely, R. A., and Millero, F. J.: The optimal carbonate dissociation
constants for determining surface water pCO₂ from alkalinity and total inorganic carbon, Marine
475 Chemistry, 65, 291–301, [https://doi.org/10.1016/S0304-4203\(99\)00021-3](https://doi.org/10.1016/S0304-4203(99)00021-3), 1999.
50. Wolf-Gladrow, D. A., Riebesell, U., Burkhardt, S., and Bijma, J.: Direct effects of CO₂



concentration on growth and isotopic composition of marine plankton, 51, 461–476,

<https://doi.org/10.1034/j.1600-0889.1999.00023.x>, 1999.

51. Zeebe, R. E. and Ridgwell, A.: Past Changes in Ocean Carbonate Chemistry, in: Past Changes
480 in Ocean Carbonate Chemistry, Oxford University Press,
<https://doi.org/10.1093/oso/9780199591091.003.0007>, 2011.

52. Zeebe, R. E. and Wolf-Gladrow, D.: CO₂ in Seawater: Equilibrium, Kinetics, Isotopes, Gulf
Professional Publishing, 382 pp., 2001.